Applied Geochemistry 102 (2019) 77–87

Contents lists available at ScienceDirect

Applied Geochemistry

journal homepage: www.elsevier.com/locate/apgeochem

Geochemical characterization of the Nirano mud volcano, Italy

Alessandra Sciarra[a,d,e,*], Barbara Cantucci[a], Tullio Ricci[a], Yama Tomonaga[b], Adriano Mazzini[c]

[a] Istituto Nazionale di Geofisica e Vulcanologia, Sezione Roma1, via di Vigna Murata 605, 00143 Rome, Italy
[b] Eawag, Swiss Federal Institute of Aquatic Science and Technology, Dübendorf, Switzerland
[c] Centre for Earth Evolution and Dynamics (CEED), University of Oslo, Norway
[d] CNR-IGAG, Consiglio Nazionale delle Ricerche- Istituto di Geologia Ambientale e Geoingegneria, Rome, Italy
[e] University of Ferrara, Department of Physics and Earth Sciences, Ferrara, Italy

ARTICLE INFO

Editorial handling by Dr M Liotta

Keywords:
Nirano mud volcano
Soil gas survey
Gas geochemistry
Thermogenic methane
Po plain

ABSTRACT

The Nirano mud volcano is located in the western sector of the Modena Apennine margin (Italy). It represents one of the most spectacular phenomena of sedimentary volcanism in the entire Italian territory and is among the largest in Europe. Here numerous aligned gryphon clusters and seeping pools constantly burst gas and mud inside a morphological depression. Besides the obvious surface expressions of these emission spots, until now the type and amount of gas released in the rest of the large Nirano caldera zone remained unknown.

An extensive geochemical soil gas survey (O_2, N_2, CO_2, CH_4, ^{222}Rn, He, H_2, and light hydrocarbons) and exhalation fluxes (CO_2 and CH_4), was carried out inside the mud volcano field with the aim of identifying soil degassing distribution, and to estimate the micro- and macro-seepage budget for both CO_2 and CH_4.

Soil gas data highlight the presence of two zones characterized by high concentrations and flux values. These enhanced seepage zones are located in the SW and NE sectors of the mud volcano suggesting that the enhanced gas emissions present in the peripheral zones, are controlled by caldera collapse structures. The most significant CO_2 flux (up to 91 g m^{-2} d^{-1}) and ^{222}Rn anomalies are located in the central part of the crater in correspondence of a morphological escarpment. Here we infer the presence of a buried tectonic system of collapsed terraces that facilitate fluids degassing. In contrast, CH_4 fluxes show a scattered distribution and low values (mean 221 mg m^{-2} d^{-1}).

Overall the CH_4 degassing budget is low (27.09 t km^{-2} y^{-1}) when compared with other Italian mud volcanoes. This could be related to a relative low emission activity during the period of the geochemical survey and to a more homogeneous dilution of surface distribution of the emission point-s.

Chemical and isotopical composition of the gas discharged from the active gryphons is methane-dominated and the thermogenic signature (ranging from −41 to −47‰) suggests a deep reservoir source. This conclusion is supported by noble-gas measurements (He, Ne, Ar, Kr, Xe) conducted in the pore water phase of the emitted mud, indicating a secondary gas exchange occurring at a depth of a few kilometers.

The geochemical anomalies found in this study, successfully predicted the occurrence of new degassing phenomena towards the NE sector of the caldera. Indeed recently (i.e. after the survey data acquisition) new manifestations of mud and gas emissions appeared in the north-eastern edge of the caldera.

1. Introduction

Mud volcanoes are the surface expression of subsurface processes characterized by movements of large masses of sediments and fluids, collectively indicated as “sedimentary volcanism” (Mazzini and Etiope, 2017). Dormant mud volcanoes are geological structures built by the surface emission of mud breccia (coarse- and fine-grained sedimentary particles and rock clasts), formation water and hydrocarbons expelled from pressurized deep sources through structurally controlled conduits (e.g., Kopf, 2002). Mazzini and Etiope (2017) highlighted two important mechanisms essential for the formation of mud volcanism: 1) gravitational instability, resulting from the fast burial of fluids and organic-rich sediments and 2) the overpressure produced by the generation of hydrocarbons at depth. The presence of efficient seals allows overpressured fluids to be entrapped in isolated geological compartments.

Mud volcanoes are worldwide diffused, particularly in active and passive margins, deep sedimentary basins related to active plate

* Corresponding author. Istituto Nazionale di Geofisica e Vulcanologia, Rome, Italy.
E-mail address: alessandra.sciarra@ingv.it (A. Sciarra).

https://doi.org/10.1016/j.apgeochem.2019.01.006
Received 13 September 2018; Received in revised form 10 January 2019; Accepted 14 January 2019
Available online 16 January 2019
0883-2927/

boundaries, as well as delta regions, or areas involving e.g. salt diapirism, as part of petroleum systems (Etiope, 2015).

In Italy, mud volcanoes occur along the external compressive margin of the Northern (Pede–Apennine margin of Emilia-Romagna) and Central Apennine (eastern Marche-Abruzzo) and in Sicily (Pellegrini et al., 1982; Capozzi et al., 1994; Martinelli, 1999; Martinelli and Judd, 2004; Etiope et al., 2007; Tassi et al., 2012). If compared to other world examples, most of the Italian mud volcanoes are small sized and seldom exhibit periodic explosions (e.g. the 2014 tragedy occurred at Macalube mud volcano in Sicily; Mazzini and Etiope, 2017, or at Santa Barbara mud volcano, Madonia et al., 2011), which are often related to important seismic activity (Accaino et al., 2007).

Nirano mud volcano (NMV), located inside the wider Regional Natural Reserve of Salse di Nirano, is distributed over an area of about 10 ha near the Nirano village (Fiorano Modenese). The number of vents present at NMV, as well as their shape and location, vary over the time (Martinelli and Judd, 2004), even if their age increases from SW to NE. Currently exist five main active sites displaying a variable number of individual active gryphons, and numerous pools. These vigorous emission points are distributed along structural alignments trending ENE-WSW and running subparallel to the Pede-Apennines thrust (Bonini, 2007, 2008). The gryphons have subcircular shape with a basal radius up to 20 m and a meter-scaled bubbling upper part that may reach up to 3 m in height. Water, mud and small fractions of liquid hydrocarbons are periodically emitted at the gryphons and pools scattered over an elliptical depression forming the volcano caldera (~500 m long, 350 m wide, ≤60 m deep) (Sciarra et al., 2015a and references therein). Discharged fluids contain also small marine fossils (calcareous nanoplankton), sub-millimetric fragments of claystones and carbonates. These represent the brecciated clasts of the formations intersected by the feeder conduit during the rise of ovepressured fluids (Bonini, 2008).

The NMV is known since ancient records and has been described by historians (Stoppani, 1873; Coppi, 1875; Pantanelli and Santi, 1896; Biasutti, 1907; Barbieri, 1947; Mucchi, 1966, 1968) and investigated for various aspects including: i) mineralogy (Ferrari and Vianello, 1985); ii) mud volcanism related to tectonic activity (Gorgoni et al., 1988; Gorgoni, 2003; Bonini, 2007, 2008, 2009; 2012; Manga and Bonini, 2012; Lupi et al., 2016); iii) geology and geomorphology (Bertacchini et al., 1999; Castaldini et al., 2003, 2005; 2007, 2011); and iv) microbiology (Heller et al., 2011, 2012; Kokoschka et al., 2015), contributing to create an important database on its evolution.

From a geochemical point of view, research surveys mainly focused on the chemical and isotopical characterization of fluids emitted by active seepage sites. Minissale et al. (2000) investigated chemical and isotopic characteristics of natural gas and thermal water of Northern Apennines, among those Nirano. They found that at NMV free gases are mainly methane (> 98%) with small amounts of other hydrocarbons, carbon dioxide and nitrogen. The carbon isotope ratios ($\delta^{13}C_{CH4} = -46‰$ PDB) indicate a thermogenic origin. Discharged waters from volcanoes are brackish (TDS = 7.12 g L^{-1}) suggesting a marine origin. Oxygen isotope ratios ($\delta^{18}O = 5.5‰$ SMOW), and hydrogen isotope ratios (δD = 4.0‰ SMOW), joint to isotopic composition of strontium and tritium, indicate negligible input of meteoric waters in the system and confirm the connate origin of the water (Cipriani et al., 2017). In this study, Minissale et al. (2000) conclude that the fluids discharged are probably syngenetic with the Plio-Pleistocene "Argille Azzurre" Formation cropping out in the study area. Moreover, the authors noted that the seeping gas is relatively enriched in helium, and suggested an enrichment in crustal radiogenic ^4He and long underground residence times. Etiope et al. (2007) reported free gas and isotopic composition of all main terrestrial mud volcanoes and other methane seeps in Italy, among those Nirano. Their results ($\delta^{13}C_{CH4} = -46‰$, $\delta^{2}H_{CH4} = -186‰$) is in agreement with Minissale et al. (2000). Heller et al. (2011, 2012) carried out chemical and microbiological analysis of mud and free gas from one of the active gryphons, founding the presence of anaerobic oxidation of methane. Tassi et al. (2012) presented gas geochemical and isotopical composition of C_2–C_{10} alkane, cyclic and aromatic compounds. They found that methane is by far the most abundant component with the presence of more than 20 different cyclic compounds with concentrations up to several μmol mol^{-1}. Cyclic compounds are likely formed by: *i)* thermal cracking and *ii)* uncompleted aromatization of alkanes occurring at depth > 3 km and temperatures not exceeding 120–150 °C.

Despite the work done, no studies have been completed to investigate the soil gas distribution in relation to possible tectonic discontinuities and characterize micro- and macro-seepage for both CO_2 and CH_4. Soil–gas geochemistry represents a widely used technique to detect seeping gases and identify preferential migration pathways and active tectonic structures such as buried faults and fractured fields (e.g. Baubron et al., 2002; Ciotoli et al., 2005, 2016; Quattrocchi et al., 2012; Sciarra et al., 2015b, 2017; 2018; Valente et al., 2018). The output of seepage is important in the framework of geogenic emissions of greenhouse gases since mud volcanoes represent the second natural source of CH_4 in the atmosphere (Etiope, 2004; Saunois et al., 2016). It is estimated that during their dormancy mud volcanoes globally emit (i.e. from seeps, gryphons and micro-seepage) 5–20 Mton y^{-1} (Mazzini and Etiope, 2017 and references therein).

The goal of our study is to fill some of the existing gaps of knowledge of the NMV presenting results of an extensive geochemical survey. More precisely this study aims to: i) define the natural degassing value (baseline or background) in the studied area, ii) identify enhanced permeability sectors possibly linked to preferential leakage pathways such as fault and/or fracture systems, iii) discriminate the migration processes and the carrier role of the various gaseous species, and, iv) quantify the CO_2 and CH_4 fluxes from soils and active cones aiming to an accurate estimation of CO_2 and CH_4 seepage output to the atmosphere.

2. Stratigraphic and geological setting

The NMV is located in the low hill territory of the Modena Apennine (Fig. 1), upon an anticline structure with a NW–SE axis associated to the Pede-Apennines thrust (e.g., Benedetti et al., 2003; Bonini, 2008). The Modena Apennine margin is characterized by prevalently compressive structures (Emilia Folds; Pieri and Groppi, 1981; Gasperi et al., 1989) produced by northbound translational movements (occurring mainly during the Messinian and Pliocene). In particular, the study area is characterized by the presence of two systems of tectonic discontinuities (fault and/or fractures) NW-SE and SW-NE oriented, respectively (Fig. 1).

The NMV develops on the bottom of a caldera-like structure, with a maximum diameter of about 500 m. The caldera collapse is believed to have formed within the Plio-Pleistocene succession (Capozzi et al., 1994; Martinelli and Rabbi, 1998; Castaldini et al., 2005; Accaino et al., 2007), possibly following different paroxysmal events of fluid and mud emission. Bonini (2008) describes this caldera as the result of the collapse of the top portion of a mud diapir arising to the surface, similarly to what happens in some submarine structures (e.g. Henry et al., 1990).

Clayey and sandy marine sediments (Argille Azzurre formation, from Middle Pliocene to Lower Pleistocene) outcrop around the NMV. These deposits overlay, from the top (Fig. 1): i) sandstones, claystones and conglomerates belonging to the Epi-Ligurian Units; ii) shales of Ligurian Units, and iii) sandstones and siltstones of Marnoso Arenacea formation (Miocene). The latter formation constitutes the deep reservoir (about 2 km depth) from which pressurized fluids migrate along high-angle thrust faults toward surface, accumulating at shallow depths within the Epi-Ligurian Units (Bonini, 2008).

3. Methodology

147 soil gas concentration (He, Ne, H_2, O_2, N_2, CH_4, CO_2, light

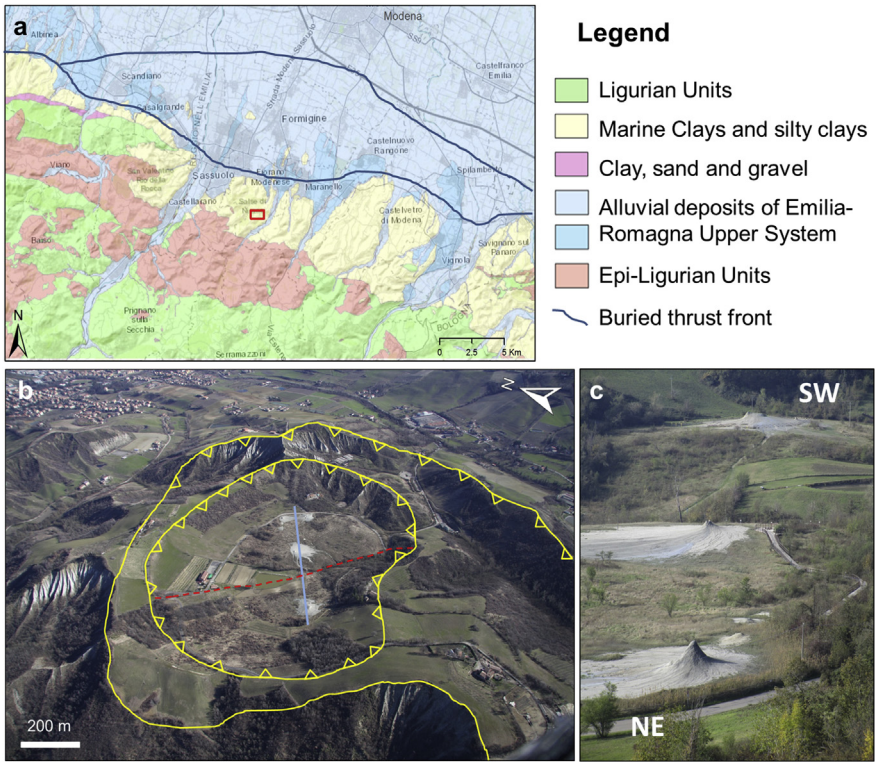

Fig. 1. a) Geological map of the Pede-Apenninic region. The Pede-Apeninne thrust is marked by the bold blue line (http://geoportale.regione.emilia-romagna.it/it/mappe); b) detailed map of NMV showing caldera ring faults (yellow line), preferential alignment of main gryphons (blue line), fault inferred by morphological evidence (dashed red line); c) picture of the gryphon clusters and their preferential NE-SW alignment. (For interpretation of the references to colour in this figure legend, the reader is referred to the Web version of this article.)

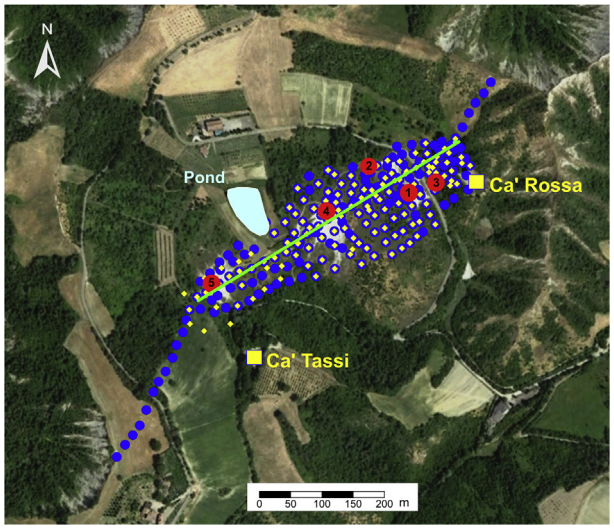

Fig. 2. Distribution of soil gas concentration (yellow diamonds), flux measurements (blue dots), SW-NE profile (green line) and location of free gas sampling on the five active sites (red dots). Ca' Tassi and Ca' Rossa are the museums of Salse di Nirano Natural Reserve. (For interpretation of the references to colour in this figure legend, the reader is referred to the Web version of this article.)

hydrocarbons and ^{222}Rn) and 209 CO_2 and CH_4 flux measurements were carried out during several surveys in spring-summer 2015 inside the NMV. To determine the soil degassing background, 18 additional flux measurements were measured outside the area that limits the mud volcanic caldera. Measurements covered an area of 78742 m^2, following a regular grid with steps of 20 and 40 m for fluxes and soil gas measurements, respectively (Fig. 2). Free gas samples were collected from five vents located in different sectors of NMV for chemical and isotopical analysis (Fig. 2).

The free gas flux was estimated by a funnel positioned above the bubbling point and connected to a 1.5 L calibrated vial through a silicon tube. The degassing was assessed measuring the time needed by the gas to replace the volume of water filling the vial. This procedure was repeated several times, in order to obtain a reliable average of the measurements.

Finally, in order to compare the results of the present study with the ones obtained by Lupi et al. (2016) by means of geoelectrical investigations, detailed fluxes and soil gas measurements were carried out along a SW-NE profile (20 m spacing between measurements) crossing five active emission structures (Fig. 2). This profile overlaps Profile 1 performed by Lupi et al. (2016) to investigate the subsurface structure of the NMV by 2D Electrical Resistivity Tomography (ERT).

3.1. Soil gas

Soil gas survey consists in collecting and analyzing gas samples from the vadose zone to measure the concentration of the gaseous species that permeate the soil pores. Sampling was accomplished in a period of stable and dry weather conditions, and in a short time to minimize any variations induced by different sampling periods. Soil gas samples were collected using a steel probe that was driven into the ground to a depth of 0.8 m, to avoid the major influence of meteorological variables (e.g., Segovia et al., 1987; Hinkle, 1994), and successively analyzed in the Fluid Geochemistry Laboratory at INGV Rome. Soil gas concentrations (He, Ne, H_2, O_2, N_2, CH_4, C_2H_2, C_2H_4, C_2H_6, CO_2) were analyzed using a MicroGC Varian 4900 CP, equipped with two Thermal Conductivity Detectors (TCD), responding to the difference in thermal conductivity between the carrier gas (He or Ar) and the sample components.

Radon (^{222}Rn; half-life 3.8 days) was analyzed directly in the field using a RAD7 Durridge alpha spectrometry instrument. The instrument is equipped with a solid-state alpha detector and it is connected with a hollow probe at depth of ~0.7 m. A single measurement has an average duration of 20 min, with partial readings every 5 min. Four measurements were completed at each site. A desiccant trap (Drierite) and an inlet filter protect the detector from soil moisture (> 10%).

3.2. CO_2 and CH_4 fluxes

CO_2 and CH_4 fluxes were measured using the "accumulation chamber" method (e.g., Chiodini et al., 1998) by means of a West System™ portable fluxmeter equipped with CO_2 and CH_4 detectors.

The CO_2 detector is a LICOR–LI820, very accurate in the range from 0 up to 600 mol m^{-2} d^{-1} (0–26400 g m^{-2} d^{-1}). The CH_4 flux meter is a TLD Tunable Laser Diode spectrometer (West System) that allows the measurement of flux in the range from 0.01 up to 750 mol m^{-2} d^{-1} (0.16–12000 g m^{-2} d^{-1}).

Data obtained directly in the field, were treated and calculated considering the variation of barometric pressure and temperature measured during the survey. The recorded concentrations measured over the time, with other parameters such as volume (0.003 m^3) and surface (0.0314 m^2) of the accumulation chamber, allow calculation of the CO_2 and CH_4 fluxes from the soil (Hutchinson et al., 2000).

3.3. Free gas

Free gases were sampled using a plastic funnel up-side-down positioned above the bubbling mud pools and connected through silicone/tygon tubes to pre-evacuated 250 mL glass flasks. Subsequently gases were analyzed using a MicroGC Varian 4900 CP. Isotopic analysis on free gas ($\delta^{13}C_{CO2}$, $\delta^{13}C_{CH4}$, $\delta^{2}H_{CH4}$, $^{3}He/^{4}He$, $^{40}Ar/^{36}Ar$) were performed by spectrometry at the laboratory of Istituto Nazionale di Geofisica e Vulcanologia, Sezione di Palermo. The $\delta^{13}C$ in CO_2 values (expressed as $\delta^{13}C_{CO2}$‰ vs. VPDB) were analyzed by mass spectrometry (Finningan Delta S). The analytical uncertainly and the reproducibility are ± 0.05‰.

The $\delta^{13}C_{CH4}$ and $\delta^{2}H_{CH4}$ values (expressed as $\delta^{13}C_{CH4}$‰ vs. VPDB and $\delta^{2}H_{CH4}$‰ vs. VSMOW, respectively) were analyzed by mass spectrometry (Varian MAT 250) according to the procedure reported by Schoell (1980). The analytical uncertainly is ± 0.15‰.

The $^{3}He/^{4}$ He ratios (expressed as R/Ra, where R is the $^{3}He/^{4}He$ measured ratio and Ra is the $^{3}He/^{4}He$ ratio in the air: 1.39×10^{-6}; Mamyrin and Tolstikhin, 1984), as well as $^{40}Ar/^{36}Ar$ ratios, were determined by using a double collector mass spectrometer (VG 5400-TFT) according to the method described by Inguaggiato and Rizzo (2004). The analytical error is ± 1%.

3.4. Noble-gas analysis in the mud pore water

Mud samples for a comprehensive noble-gas analysis (i.e., He, Ne, Ar, Kr, Xe as well as the $^{3}He/^{4}He$, $^{20}Ne/^{22}Ne$, and $^{36}Ar/^{40}Ar$ isotope ratios) in the water phase were collected in copper tubes sealed airtight by two metal clamps (Brennwald et al., 2003, 2013; Tomonaga et al., 2011, 2013, 2014, 2015; Tyroller et al., 2016). Sample preparation in the laboratory was carried out according to the method of Tomonaga et al. (2011). The copper tube containing each sample was divided into two aliquots by placing four additional metal clamps. Each aliquot was then centrifuged to separate the water from the sediment. After the centrifuging process, one aliquot was pinched off at a position located slightly above the sediment-water interface, which was determined by visual inspection by opening the copper tube of the other aliquot (Tomonaga et al., 2011). Noble-gas analysis was conducted only on the separated water according to the well-established experimental protocols commonly used to determine noble-gas abundances in water samples at the Noble Gas Laboratory of ETH Zurich (Beyerle et al., 2000).

3.5. Data treatment

Preliminary analysis involved the calculation of standard statistical parameters to evaluate the basic characteristics of the data, define a background value and its anomaly threshold. Therefore, to identify statistical populations for each parameter, all collected data were processed with a statistical approach, by means of normal probability plot (NPP). According to Sinclair (1974, 1991), the NPP provides a good method to distinguish different populations and a more objective approach to statistical anomaly threshold estimation (Ciotoli et al., 2007).

On the basis of NPP classification contour maps of investigated gas species were elaborated by kriging interpolation method (e.g., Bergfeld et al., 2001), derived from empirical semivariograms.

The acquired flux measurements were used to estimate the total output (Q) of the CO_2 and CH_4 directly discharged by soil according to Chiodini and Frondini (2001) approach (Eq. (1)). The emission rates (expressed in tday $^{-1}$) were calculated by summing the contribution of each population, computed by multiplying the mean flux value for the area covered by each population (Eq. (1)). The budget calculation does not consider the amount due to the soil respiration component (background) and vent emissions (macroseeps).

$$Q_{CO_2,CH_4} = \sum \Phi_{CO_{2,i;}} \Phi_{CH_{4,j}} \times A_{i,j} \quad (1)$$

where $\Phi_{CO_{2,i}}$ represents the average φ_{CO_2} of the i-th population, $\Phi_{CH_{4,j}}$ represents the average φ_{CH_4} of the j-th population, and $A_{i,j}$ is the calculated area covered by each population.

4. Results and discussion

The main statistics of sampled data are reported in Table 1. N_2 and O_2 were not reported in Table 1 and discussed as their average values match essentially the atmospheric composition (i.e., 20.95 vol% and 78.08 vol%, respectively; Hermansson et al., 1991; Etiope and Lombardi, 1995).

Statistical parameter of φCH_4, CH_4, ^{222}Rn and φCO_2 (Table 1) have a dispersed distribution as highlighted by the high values of standard deviation (2547.5, 624.3, 6125.3 and 12.9, respectively). On the other hand, φCO_2, ^{222}Rn and CH_4 show high skewness values (2.15, 2.66 e 3.86, respectively), suggesting the presence of outliers. The φCH_4 and, to a lesser extent, He and H_2 have a skewness value (13.55, 4.84 and 5.48, respectively) showing a clear dispersed distribution with anomalous values.

Table 1
Descriptive statistics of CO_2 and CH_4 fluxes, and soil gas concentration of He, Ne, H_2, CH_4, CO_2 and ^{222}Rn measured in the NMV area.

	φCO_2 (g m^{-2} d^{-1})	φCH_4 (mg m^{-2} d^{-1})	He (ppmv)	Ne (ppmv)	H_2 (ppmv)	CH_4 (ppmv)	CO_2 (vol%)	^{222}Rn (Bq m^{-3})
N	227	227	147	147	147	147	147	147
Mean	17.9	220.9	5.83	13.3	2.7	290.9	0.92	3362
Median	16.68	0.01	5.5	13.8	1.4	21.4	0.78	838
Minimum	0.00	−7.27	2.8	2.85	0.08	0.44	0.04	0.00
Maximum	91.41	3208.5	17.9	26.9	38.8	6212.1	5.5	28800
LQ	9.33	0.003	5.2	12.4	0.9	4.6	0.3	202
UQ	22.7	0.028	6.3	15.3	2.7	355.8	1.1	2625
Variance	165	6489667	1	19	20	389744	1	37519204
Std. dev.	12.9	2547.5	0.9	4.3	4.5	624.3	0.86	6125.3
Skewness	2.15	13.55	4.84	−0.16	5.48	3.86	2.58	2.66

4.1. Soil gas concentrations

The distribution of soil gas, in particular trace gases as ^{222}Rn, He and H_2, was investigated to identify potential faults and/or fractures related to preferential migration pathways and the possible interaction between deep reservoirs and surface.

Normal probability plots were used to identify background, anomalous and outliers values. In particular values above 2 vol% for CO_2, 10 ppmv for H_2, 40 ppmv for CH_4, 2500 Bq m^{-3} for Rn, 5.5 ppmv for He and 18 ppmv for Ne have been considered as anomalous.

The main statistical parameters of Rn, CO_2, CH_4 and He data collected in the NMV were compared to those measured in the cultivated areas of Modena Province (Sciarra et al., 2013) and obtained by the same methodology, in order to have a homogeneous database as a reference.

Concentrations of radon and carbon dioxide show mean and median that are lower compared to reference values. In particular, mean ^{222}Rn values for NMV are 3362 Bq m^{-3} versus 4800 Bq m^{-3}, while CO_2 concentration has a mean of 0.92 vol% with respect to 2.31 vol% of reference values.

On the contrary, methane concentrations are about two orders of magnitude higher than reference values, with mean of 290 ppmv and median of 21.4 ppmv versus 6.01 and 0.15 ppmv, respectively, and H_2 is about one order of magnitude higher (2.7 and 1.4 ppmv) than those reported by Sciarra et al. (2013; 0.44 and 0.31 ppmv). The He mean concentration (5.83 ppmv) substantially agrees with both atmospheric and reference values.

Spatial distribution of CO_2 (Fig. 3a) shows anomalous values (> 2 vol%) in the NE sector of the study area, where the mud volcano activity is more recent (west to Ca' Rossa museum). Other weak high values are present in the central part of the crater zone close to a large water pond.

Contour map of ^{222}Rn (Fig. 3b) highlights two zones in the NMV characterized by high values (> 14000 Bq m^{-3}). The first one is located in the NE area, in correspondence of a CO_2 anomaly while the second is located in the SW of the survey area, between the southwesternmost gryphon site (point 5) and the water pond.

CH_4 and He (Fig. 3c and e) show a similar spatial distribution, with high values (> 2500 ppmv and 6 ppmv, respectively) in the northern part of the study area (points 2 and 4) and close to Ca' Rossa (point 3). This observation suggests that both gas species may be sourced from the same layer, with methane acting as carrier.

H_2 anomalous values (> 16 ppmv) are distributed in three distinct areas located in the NE, N and SW areas in agreement with higher values of the other gas species (Fig. 3d).

The Ne distribution (Fig. 3f) shows a preferential alignment of anomalous values along the oblique line crossing the study area from SW to NE. This gas species is indicative of circulation path of shallower fluids probably linked to a surficial fracturation system.

Spatial distribution of the highest values for CO_2, ^{222}Rn, CH_4, He, Ne and H_2 highlights a general association among the considered species in the NE sector of the studied area, whereas ^{222}Rn, Ne, H_2 show a good correlation also in the SW sector.

These two regions are located at the extremities of the NE-SW aligned seepage sites and coincide with the morphological edges of the caldera. We suggest that these preferential locations may result from: 1) a sealing effect by the mud mostly extruded in the central part, and/or 2) by a tectonic control operated by the caldera collapse faults that facilitate the preferential rise of deep fluids. A similar mechanism has been already suggested for other mud volcano sites (Mazzini et al., 2009; Mazzini and Etiope, 2017).

Since ^{222}Rn and other trace gases (He and H_2) are considered suitable fault tracers and CO_2 and CH_4 are believed to act as carriers for these gases (Beaubien et al., 2003; Sciarra et al., 2015b, 2017; 2018; Ciotoli et al., 2016), their association suggests the presence of two areas characterized by high permeability zones from which gas upraise at surface.

4.2. CO_2 and CH_4 flux measurements

Statistical elaboration on the basis of NPP allowed to define threshold anomaly for φCO_2 (20 g m^{-2} d^{-1}), and φCH_4 (44 mg m^{-2} d^{-1}).

The average CO_2 exhalation flux (Table 1) reveals values lower than those measured in cultivated areas of the Modena Province (17.9 vs. 21.9 g m^{-2} d^{-1}; Sciarra et al., 2013). The highest values are located in the NE sector of the study area, where the mud volcano activity is more recent (around Ca' Rossa) and in the central part of the area, in correspondence of the water pond and the morphological slope. A focused anomaly is located in the SW edge of the NMV (Fig. 4a). Flux measurements performed outside the area hosting the mud volcano (blue dots in Fig. 4a) range from 4 to 20.22 g m^{-2} d^{-1}, within the background values of those measured inside the crater zone.

Methane micro-seepage shows average values significantly lower than those measured in cultivated areas of the Modena Province (220 vs. 670 mg m^{-2} d^{-1}; Sciarra et al., 2013). The highest values (from 400 to 3200 mg m^{-2} d^{-1}) are distributed along the oblique axis crossing the area with a NE-SW trend. Flux measurements performed outside the NMV (blue dots in Fig. 4b) are characterized by background values ranging from 2.38 to 42.61 mg m^{-2} d^{-1}.

The total gas emission rates over the surveyed surface (A_{tot} = 0.0787 km^2) have been computed following the Chiodini and Frondini (2001) approach (Eq. (1)). Results give 299.3 t y^{-1} for CO_2 (Q_{CO_2}) and 2.13 t y^{-1} for CH_4 (Q_{CH_4}).

The free gas flux, measured for the most recent active seeps at point 3 (Fig. 5), revealed an emission rate of 64.8 L h^{-1} (or 1.8×10^{-5} m^3 s^{-1}) constituted by 97% of CH_4 and 1% of CO_2 (see Section 4.4). The daily emissions from the gryphon to the atmosphere are 3.299×10^{-5} t d^{-1} for CO_2 and 1.08×10^{-3} t d^{-1} for CH_4. By considering emissions from other 11 historically stable active gryphons and pools that visually have a qualitatively similar degassing mode, we obtained a macroseep output of 0.14 t y^{-1} for CO_2 and 4.72 t y^{-1} for CH_4.

Etiope et al. (2007) estimated the CH_4 output of Nirano from macroseeps (gryphons, bubbling pools and dry seeps) and microseepage (soil diffuse degassing). Their measured macroseepage is slightly higher than the one obtained in this study (6 t y^{-1} vs. 4.72 t y^{-1}), whereas the microseepage output is about one order of magnitude higher (i.e. 26.4 t y^{-1} vs. 2.13 t y^{-1}). This difference may be due to the distinct investigation periods or due to the different sampling density (6 measurements within 10000 m^2 vs. 210 measurements within 78742 m^2 of this study – a difference of almost one order of magnitude). Indeed, the fluid emissions and mud activities change over the time.

Our results emphasize that sampling density may affect the observed soil gas distribution (e.g., Ciotoli et al., 2007). At high resolution scale, when sampling is performed within the influence "domain" (spatial range) of a structure, the gas behavior is less apparent than at the regional scale, highlighting the different contribution of phenomena acting along specific directions (i.e., fault-related anisotropy) versus those acting randomly (i.e., isotropic field of background). Nevertheless, channeling phenomena (preferential pathways), can be clearly seen by high resolution surveys because of their very close spatial influence. Coupled regional and high-resolution sampling provides information about the spatial influence of the structural features on the soil gas data (Ciotoli et al., 2007).

Finally, it is important to note that Etiope et al., (2007) carried out measurements only in the flank of gryphons (personal communication), whereas for this study the whole caldera area was sampled. The flanks of gryphons are typically affected by significant macroseepage manifestations therefore resulting in a overall higher flux estimate.

With respect to other Italian mud volcanoes, the Nirano CH_4 macro and microseepage estimated in this study are lower than those

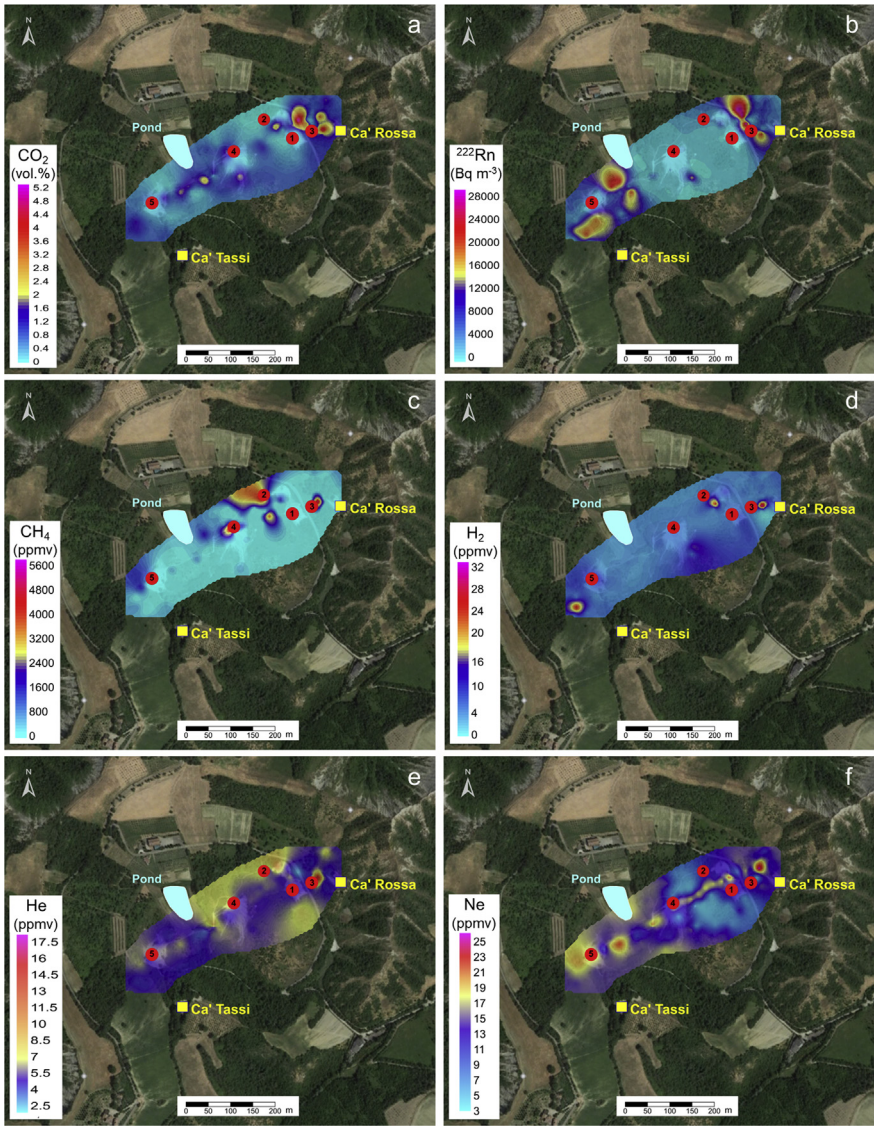

Fig. 3. Contour maps for the concentrations of investigated gas species: a) CO_2; b) ^{222}Rn; c) CH_4; d) H_2; e) He; f) Ne, show the presence of high soil gas values at the edges of the caldera, a good spatial correlation between trace gas elements and their carrier gasses, and along the NE-SW aligned gryphons distribution.

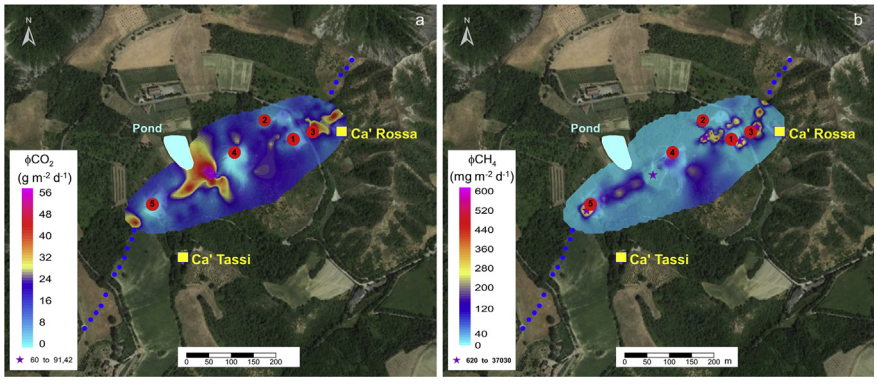

Fig. 4. Distribution of flux measurements for a) φCO_2 and b) φCH_4 highlight the presence of more intense degassing in coincide with the morphological edges and the slope of the caldera.

Fig. 5. Active seepage sites at the NMV. a-b) landscape, c-d) particular of bubbling phenomenon from sampling points 4 and 2, respectively, e) mud pool of point 3, f) point 1, g-h) point 5.

Table 2
Output of φCH_4 from macroseeps and microseeps.

Site	Area (m^2)	N. Vents	Macroseep output (t y^{-1})	Microseepage output (t y^{-1})	N. meas. microseepage	Output (t y^{-1})
Regnano[a]	5800	8	5	29	11	34
Nirano[a]	10000	18	6	26.4	6	32.4
Macalube[a]	1400000	69	20	374	9	394
Nirano (this study)	78742	12	4.72	2.13	210	6.85

[a] From Etiope et al. (2007).

estimated for Regnano (5 t y^{-1} and 29 t y^{-1}, respectively; Table 2), located about 20 km far to Nirano and about one order of magnitude lower than Macalube (Sicily; Table 2).

4.3. SW-NE oblique profile

Detailed fluxes and soil gas measurements (20 m spaced) were carried out along a 550 m long profile intersecting five active mud emission areas. The SW-NE oriented profile (Fig. 2) follows Profile 1 performed by Lupi et al. (2016) using 2D Electrical Resistivity Tomography (ERT).

In order to highlight the trend of different gas species and find similarities in their spatial distribution, soil gas concentrations and flux profiles were compared with the ERT data (Fig. 6).

φCO_2, CO_2, He and ^{222}Rn show high values in the sectors between 80 and 230 m. This interval is characterized by a prominent 15 m high escarpment with NW-SE orientation, likely related to subsidence dynamics ongoing in the central area. The presence of these tectonic structures is likely facilitating the gas uprising.

Anomalous values of CO_2, He, ^{222}Rn, H_2 and φCH_4 are also concentrated between 400 m (gryphon 1) and the end of the profile where new mud emissions appeared in October 2015.

In contrast, H_2, CH_4 and φCH_4 show high values between 0 and 70 m, and around 10–20 m is present a good correlation among He, ^{222}Rn, H_2 and CH_4 (i.e. in the area around gryphon 5).

The highest soil gas concentrations positively correlate with the three dome-shaped conductive anomalies mapped by Lupi et al. (2016) at ~20 m depth. Unfortunately, the geochemical and geophysical datasets of Lupi et al. (2016) have not been acquired at the same time and, in addition, the area investigated through the ERT survey would not permit an spatial analysis. However, the quantitative amplitude of the anomalies was only used as a way to detect qualitatively enhanced permeability sectors possibly linked to preferential leakage pathways.

Depending on the combination of gas species anomalies, it is possible to distinguish if these are related to local conditions (e.g. lithology, permeability), or to gas uprising along preferential pathways. Soil gas distributions suggests the presence of sectors characterized by high permeability where CO_2 and CH_4 play a dominant role as carrier gases for advective transport and redistribution of trace gases (e.g., He, ^{222}Rn, H_2). Indeed, Martinelli and Judd (2004) suggest that the decay rate of ^{226}Ra to ^{222}Rn does not vary with time, so changes in the ^{222}Rn emission rate must result from variations in the expulsion velocity of the fluids. The fluids are confined within the source rocks, consequently changes in the pore pressure caused by crustal movements explain the variations in fluid expulsion velocity (Martinelli and Judd, 2004).

4.4. Free gases emitted from the gryphons

Five active gryphons were sampled for free gas chemical and isotopical analysis (Fig. 2) and the analytical results are presented in

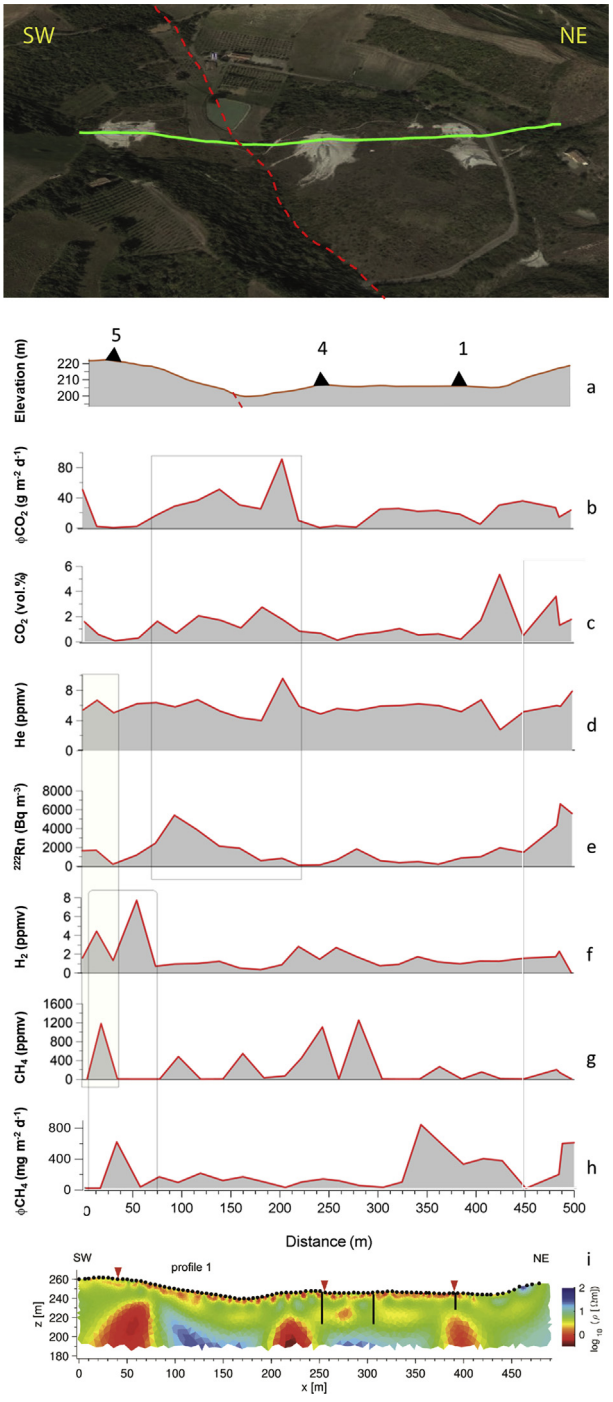

Fig. 6. Google Earth image of the oblique SW-NE profile (green line), the inferred fault (red dashed line) described in Fig. 1, with the completed measurements of: a) vertically exaggerated topography profile (black triangles indicate the position of the main gryphon clusters), b) φCO_2, c) CO_2, d) He, e) ^{222}Rn, f) H_2, g) CH_4, h) φCH_4, i) ERT profile 1 (Lupi et al., 2016). (For interpretation of the references to colour in this figure legend, the reader is referred to the Web version of this article.)

Table 3.

The seeping gas is methane-dominated, typically with concentrations higher than 90%, CO_2 content ranging from 0.5 to 8 vol% and light hydrocarbons (C_2H_6) ranging from 90 to 3350 ppmv.

The isotopic composition of the sampled gas shows an argon isotopic ratios of 307–323 being slightly higher compared to the atmospheric air value ($^{40}Ar/^{36}Ar$ = 298.56; Lee et al., 2006) indicating an enrichment in radiogenic ^{40}Ar (also observed in the mud pore water; see Section 4.5, Table 4). The $^{3}He/^{4}He$ ratio of about 0.02 Ra suggests a crustal origin (Mamyrin and Tolstikhin, 1984) as well as the He/Ne ratio (ranging from 57 to 116; Bertrami et al., 1984). Isotopic values of methane for sites 1, 3, 5 (Fig. 2) show $\delta^{13}C_{CH4}$ and $\delta^{2}H_{CH4}$ values ranging from −47.5 to −41.4‰ VPDB, and from −184 to −177‰ VSMOW, respectively. These values suggest a thermogenic origin of CH_4 as graphically reported in Fig. 7. In the revised $\delta^{13}C_{CH4}$ vs. $\delta^{2}H_{CH4}$ diagram (Milkov and Etiope, 2018), Nirano data were compared to soil gas sampled before and after the 2012 Emilia seismic sequence (Sciarra et al., 2017) and other mud volcanoes in the Emilia Romagna Region. The comparison highlights the different origin of Nirano gas with respect to the other gas on the Modena province. Indeed, the thermogenic origin of CH_4 is ascribed to the decomposition of organic matter in sediments buried at more than 3000 m depth where the temperatures are higher than 100 °C (e.g., Whiticar and Suess, 1990; Tassi et al., 2012). The results of this study are therefore in good agreement with those reported in the literature for most part of Italian mud volcanoes (Minissale et al., 2000; Capozzi and Picotti, 2002; Grassa et al., 2004; Etiope et al., 2007; Tassi et al., 2012). Moreover, on the basis of the revised diagram, NMV and Puianello samples (magenta and green stars, respectively, in Fig. 7) highlight also a possible secondary microbial gases origin.

The isotopic values of $\delta^{13}C_{CO2}$ (≈21‰ VPDB) suggest an origin due to anaerobic oxidation of heavy hydrocarbons (Pallasser, 2000), often followed by secondary methanogenesis. This is especially true for gas samples characterized by $\delta^{13}C_{CO2}$ values higher than 10‰ V-PDB (Tassi et al., 2012). Depending on microbial communities and physic-chemical conditions of the reservoir (Wang et al., 2005), methanogenesis process are able to strongly enrich the residual CO_2 in ^{13}C (Etiope et al., 2009). In order to verify the genetic field and the main process affecting the studied gasses, the $\delta^{13}C_{CH4}$ versus C_1/C_{2+} diagram (Fig. 8A) and $\delta^{13}C_{CH4}$ versus $\delta^{13}C_{CO2}$ diagram (Fig. 8B) were plotted. Both diagrams confirm what already indicated by the $\delta^{13}C_{CH4}$ vs. $\delta^{2}H_{CH4}$ diagram, pointing to a secondary microbial gases, produced during methanogenesis resulting in ^{13}C enriched CO_2 ($\delta^{13}C$ > 2‰ and up to +31‰ at Puianello site).

4.5. Noble gases in the pore water of the extruded mud

Noble gas analyses conducted in the pore water of two sampled vent sites are reported in Table 4.

Sample NIR16-03 appeared to be contaminated by air, as all measured concentrations are much higher than the concentrations expected for air-saturated water (ASW) for the temperature of the mud during the sampling (11.0 °C). It is possible to perform a very simple correction for air contamination based on the Ne excess with respect to the expected saturation concentrations. As Ne originates mainly from the atmosphere and its solubility is rather low, air contamination results in a super-saturation with respect to the expected solubility equilibrium concentration begin larger than the super-saturation for the heavier noble gases (Ar, Kr, and Xe). Thus, Ne is among all noble gases the most suitable proxy to quantify air contamination based on a single gas species. The saturation concentration of Ne at the temperature of the collected mud (11.0–12.8 °C) is about $1.9{\cdot}10^{-7}$ cm^{3}STP/g. Hence, the measured Ne concentration in sample NIR16-03 of $155{\cdot}10^{-7}$ cm^{3}STP/g is in excess of $153{\cdot}10^{-7}$ cm^{3}STP/g with respect to the equilibrium concentration. The volume fraction of Ne in atmospheric air is $1.818{\cdot}10^{-5}$ (Ozima and Podosek, 2002). Therefore, the volume of air necessary to produce the measured Ne excess is about 0.85 cm^{3}STP/g We used this estimation to determine the original $^{3}He/^{4}He$ ratio in the pore water of $3.0{\cdot}10^{-7}$ (i.e., 0.22 Ra) which is close to the value determined for sample NIR16-04 of $1.5{\cdot}10^{-7}$ (i.e., 0.11 Ra). These similar He isotope ratios indicate that a large share of He is radiogenic and originates from the decay of U and Th in the Earth's crust. This interpretation is in agreement with the measurement performed in the free

Table 3
Chemical and isotopic analysis of free gas collected from 5 active gryphons in May 2015 and March 2016(*), and from Puianello mud volcano (gryphon 6).

Gryphon	He (ppmv)	Ne (ppmv)	H_2 (ppmv)	CH_4 (vol%)	CO_2 (vol%)	C_2H_6 (ppmv)	$\delta^{13}C_{CO2}$ (VPDB)	$\delta^{13}C_{CH4}$ (VPDB)	$\delta^{2}H_{CH4}$ (VSMOW)	Rc/Ra	He/Ne	$^{40/36}Ar$
1	12.7	10.5	4.1	97.92	2.1	660	13.5	−47.5	−182			
1B	21.3	0.19	3.19	99.23	0.72	456	21.1	−41.4	−182	0.021	100.52	323.3
2	7.31	11.25	1.5	99.43	0.51	129						
3*	20.4	2.85	1.92	98.94	1.1	636	21.86	−47.22	−177.3	0.02	57.2	307.1
4	7.78	11.62	1.46	91.34	8.64	89						
5	23.2	12.3	8	99.36	0.76	95						
5B*	34.82	13.82	6.06	98.97	1.01	274	21.4	−46.7	−184			
6	30.1	0.26	1.48	95.38	3.28	3350	31.3	−46.2	−184	0.03	115.68	306.3

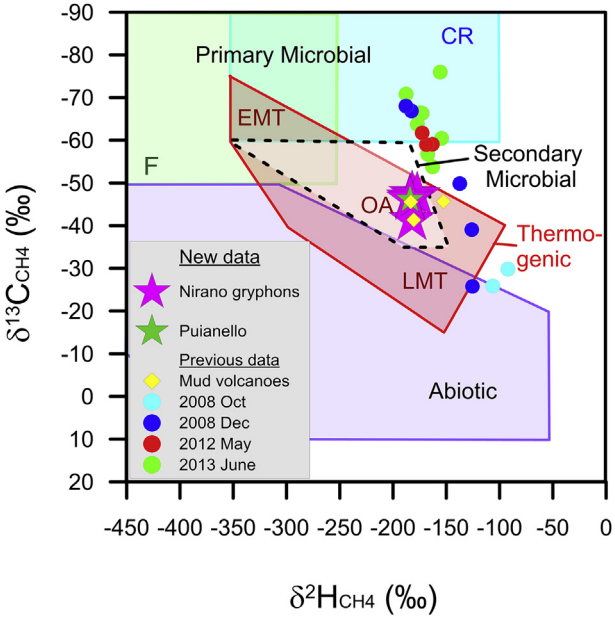

Fig. 7. Methane genetic diagram of $\delta^{13}C_{CH4}$ vs. $\delta^{2}H_{CH4}$ for free gas sampled in active gryphons of NMV (magenta stars) after Milkov and Etiope (2018). Green stars: free gas sampled in Puianello gryphon; light blue and blue dots: soil gas sampled in Modena Province in 2008; red dots and green diamonds: soil gas collected during and after the 2012 Emilia seismic sequence (Sciarra et al., 2017). Yellow diamonds: free gas sampled in other mud volcanoes in the Emilia Romagna Region (Etiope et al., 2007). CR – CO_2 Reduction; F – fermentation; G – geothermal, hydrothermal, crystalline; A – abiotic; EMT – early mature thermogenic gas; OA – oil-associated thermogenic gas; LMT – late mature thermogenic gas. (For interpretation of the references to colour in this figure legend, the reader is referred to the Web version of this article.)

gas phase (see Section 4.4) showing $^{3}He/^{4}He$ ratios significantly lower than the air value (i.e., about 0.02 Ra).

Sample NIR16-04 shows atmospheric noble gas concentrations being lower than the expected ASW values calculated for the mud temperature recorded during the sampling campaign (12.8 °C). Degassing (or re-equilibration) during sampling is not likely, as the sample has been acquired in March when the average air temperature was even lower than the mud temperature. Therefore, the general noble-gas depletion observed for sample NIR16-04 indicates that secondary gas exchange occurred with a free gas phase at depth. In light of the gas composition discussed in Section 4.4, it is reasonable to assume that this free gas phase is mainly composed by thermogenic methane produced at depths of a few kilometers, secondary altered by biodegration processes. The preservation of the signature produced by secondary gas exchange at possibly high temperatures suggests that the interaction of the mud with shallower fluids is of minor importance.

5. Conclusions

A geochemical survey including 227 CO_2 and CH_4 flux sites and 147 CO_2, CH_4, Rn, He, H_2 and light hydrocarbons concentration measurements has been carried out inside the NMV in order to investigate the gas seepage from soil and estimate the CO_2 and CH_4 output. Moreover, free gas for chemical and isotopic analysis was collected from five active sites located in different sectors of the volcano.

The main active gryphons and seeps are distributed along a 500 m long SW-NE oriented alignment that is likely controlled by a tectonic structure providing pathway for the rise of deep fluids. Results show that on average Rn activity, CO_2 concentration, ϕCO_2 and ϕCH_4 are lower than those measured in cultivated areas of the Modena province, whereas CH_4 concentrations are higher.

The distribution of trace elements such as ^{222}Rn, He, and H_2 were studied in order to identify potential faults and/or fractures related to preferential migration pathways and the possible interactions between reservoir and surface. Anomalous ϕCO_2 and ϕCH_4, Rn activities and CO_2, CH_4, He, H_2 concentrations, observed in the two regions at the edge of the NMV (NE and SW), indicate the presence of high permeability areas. Here tectonic structures controlling the collapse of the caldera are interpreted to be the preferential leakage pathways for the migrating gas. Other anomalies (ϕCO_2) are located along a

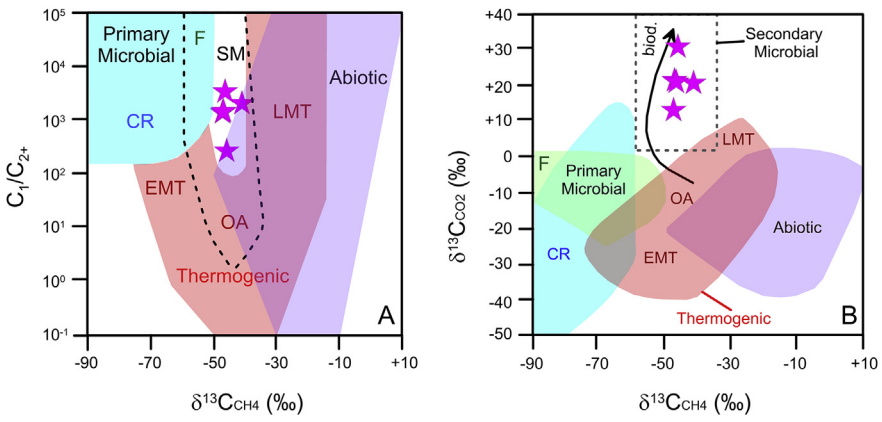

Fig. 8. Genetic diagram of $\delta^{13}C_{CH4}$ vs. C_1/C_{2+} (A) and $\delta^{13}C_{CH4}$ vs. $\delta^{13}C_{CO2}$ (B) for free gas sampled in active gryphons of NMV (magenta stars) and Puianello gryphon (green star), after Milkov and Etiope (2018). CR – CO_2 Reduction; F – fermentation; G – geothermal, hydrothermal, crystalline; A – abiotic; EMT – early mature thermogenic gas; OA – oil-associated thermogenic gas; LMT – late mature thermogenic gas; SM – secondary microbial. (For interpretation of the references to colour in this figure legend, the reader is referred to the Web version of this article.)

Table 4
Noble-gas concentrations and isotope ratios measured in the water phase of the mud collected at gryphons 5 and 3. The concentrations are given in cm^3STP (STP: standard temperature and pressure of 0 °C and 1 bar, respectively) per gram of water.

Samples	He	Ne	Ar	Kr	Xe	$^3He/^4He$	$^{20}Ne/^{22}Ne$	$^{36}Ar/^{40}Ar$
	[10^{-7} cm^3STP/g]	[10^{-7} cm^3STP/g]	[10^{-4} cm^3STP/g]	[10^{-8} cm^3STP/g]	[10^{-8} cm^3STP/g]	[10^{-6}]	[-]	[10^{-3}]
NIR16-03 (Gryphon 5)	49.9 ± 0.3	155 ± 2	83 ± 4	95 ± 1	7.00 ± 0.07	1.26 ± 0.02	9.80 ± 0.01	3.1 ± 0.1
NIR16-04 (Gryphon 3)	1.75 ± 0.01	0.37 ± 0.01	0.57 ± 0.01	1.24 ± 0.02	0.19 ± 0.01	0.15 ± 0.01	9.3 ± 0.1	3.46 ± 0.05

morphological slope in the central part of the crater suggesting that the observed morphological escarpment has a tectonic control for gas migration.

Estimated CH_4 micro and macro-seepage values are lower than those measured during previous surveys in the NMV and in other areas of Po Plain. This suggests that the NMV is in a relative quiescent activity period where lower gas emissions from active gryphons are associated with a wider spatial distribution.

The extruded gas is methane-dominated with minor amounts of nitrogen, oxygen, carbon dioxide, and ethane. Isotopic analyses highlight the thermogenic origin of emitted methane which original signature was altered by biodegradation processes. Noble-gas elemental and isotopic signatures constrain the crustal origin of these emissions.

Soil gas monitoring allowed to constrain the relationship between geochemistry and tectonics, and permitted the identification of areas with high permeability such as the NE area of the crater zone where new active mud emissions occurred after the data acquisition of this survey. This newly born site represents today the most active seepage phenomena at the NMV. Potentially other eruptive phenomena could be expected in the future following the same NE trend.

Acknowledgements

A.M. was financially supported by the European Research Council under the European Union's Seventh Framework Programme Grant agreement n 308126 (LUSI LAB project, PI A. Mazzini). We acknowledge the support from the Research Council of Norway through its Centers of Excellence funding scheme, Project Number 223272 (CEED). Field surveys were supported by Fiorano Municipality in collaboration with UNIMORE (Accordo di ricerca tra il Comune di Fiorano Modenese e il Dipartimento di Scienze Chimiche e Geologiche dell'Università di Modena e Reggio Emilia).

Appendix A. Supplementary data

Supplementary data to this article can be found online at https://doi.org/10.1016/j.apgeochem.2019.01.006.

References

Accaino, F., Bratus, A., Conti, S., Fontana, D., Tinivella, U., 2007. Fluid seepage in mud volcanoes of the northern Apennines: an integrated geophysical and geological study. J. Appl. Geophys. 63, 90–101.
Barbieri, G., 1947. Nuove osservazioni sulle salse emiliane. Riv. Geogr. Ital. 54, 172–185.
Baubron, J.C., Rigo, A., Toutain, J.P., 2002. Soil gas profiles as a tool to characterise active tectonic areas: the Jaut Pass example(Pyrenees, France). Earth Planet. Sci. Lett. 196, 69–81.
Beaubien, S.E., Ciotoli, G., Lombardi, S., 2003. Carbon dioxide and radon gas hazard in the Alban Hills area (central Italy). J. Volcanol. Geoth. Res. 123, 63–80.
Benedetti, L.C., Tapponnier, P., Gaudemer, Y., Manighetti, I., Van der Woerd, J., 2003. Geomorphic evidence for an emergent active thrust along the edge of the Po Plain: the Broni-Stradella fault. J. Geophys. Res., v. 108, 2238. https://doi.org/10.1029/2001JB001546.
Bergfeld, D., Goff, F., Janik, C.J., 2001. Elevated carbon dioxide flux at the Dixie Valley geothermal field, Nevada: relations between surface phenomena and the geothermal reservoir. Chem. Geol. 177 (1–2), 43–66.
Bertacchini, M., Giusti, C., Marchetti, M., Panizza, M., Pellegrini, M. (Eds.), 1999. I beni geologici della Provincia di Modena, Artioli Ed. Modena, pp. 104.
Bertrami, R., Ceccarelli, A., Lombardi, S., 1984. L'elio dei gas del suolo nella prospezione geotermica. Rend. Soc. Ital. Mineral. Petrogr 39, 331–342.
Beyerle, U., Aeschbach-Hertig, W., Imboden, D.M., Baur, H., Graf, T., Kipfer, R., 2000. A mass spectrometric system for the analysis of noble gases and tritium from water samples. Environ. Sci. Technol. 34, 2042–2050.
Biasutti, R., 1907. Le salse dell'Appennino settentrionale. Mem. Geogr. II 101–255.
Bonini, M., 2007. Interrelations of mud volcanism, fluid venting, and thrust-anticline folding: examples from the external northern Apennines (Emilia-Romagna, Italy). J. Geophys. Res. 112, B08413. https://doi.org/10.1029/2006JB004859.
Bonini, M., 2008. Elliptical mud volcano caldera as stress indicator in an active compressional setting (Nirano, Pede-Apennine margin, northern Italy). Geology 36, 131–134.
Bonini, M., 2009. mud volcano eruptions and earthquakes in the northern Apennines and sicily, Italy. Tectonophysics 474, 723–735.
Bonini, M., 2012. Mud volcanoes: indicators of stress orientation and tectonic controls. Earth Sci. Rev. 115, 121–152.
Brennwald, M.S., Hofer, M., Peeters, F., Aeschbach-Hertig, W., Strassmann, K., Kipfer, R., Imboden, D.M., 2003. Analysis of dissolved noble gases in the pore water of lacustrine sediments. Limnol Oceanogr. Methods 1, 51–62.
Brennwald, M.S., Vogel, N., Scheidegger, Y., Tomonaga, Y., Livingstone, D.M., Kipfer, R., 2013. Noble gases as environmental tracers in sediment porewaters and in stalagmite fluid inclusions. In: Burnard, P. (Ed.), The Noble Gases as Geochemical Tracers. Advances in Isotope Geochemistry. Springer, Berlin, Heidelberg, pp. 123–153.
Capozzi, R., Picotti, V., 2002. Fluid migration and origin of a mud volcano in the Northern Apennines (Italy): the role of deeply rooted normal faults. Terra. Nova 14, 363–370.
Capozzi, R., Menato, V., Rabbi, E., 1994. Manifestazioni superficiali di fluidi ed evoluzione tettonica recente del margine Appenninico Emiliano-Romagnolo: indagine preliminare. Atti Ticinensi Scienze Terra 1, 247–254.
Castaldini, D., Chiriac, C., Ilies, D.C., Barozzini, E., 2003. Documenti digitali per la conoscenza integrata dei Geositi: l'esempio della Riserva Naturale delle Salse di Nirano. In: Piacente, S., Poli, G. (Eds.), La Memoria Della Terra. Regione Emilia Romagna. L'inchiostro blu, Bologna, pp. 121–127.
Castaldini, D., Valdati, J., Ilies, D.C., Chiriac, C., Bertogna, I., 2005. Geo-tourist map of the natural Reserve of salse di Nirano (Modena Apennines, northern Italy). Il Quat. 18, 245–255.
Castaldini, D., Conti, S., Conventi, M., Dallai, D., Del Prete, C., Fazzini, M., Fontana, D., Gorgoni, C., Ghinoi, A., Russo, A., Sala, L., Serventi, P., Verri, D., Barbieri, M., 2007. Le Salse di Nirano. CD ROM. Enciclopedia Multimediale. Comune di Fiorano Modenese.
Castaldini, D., Conventi, M., Coratza, P., Liberatoscioli, E., 2011. La "nuova" carta turistico - ambientale della Riserva naturale regionale delle salse di Nirano (appennino modenese, italia settentrionale). Bollettino A.I.C. nr 143/2011, I275–I289.
Chiodini, G., Frondini, F., 2001. Carbon dioxide degassing from the Albani Hills volcanic region, Central Italy. Chem. Geol. 177, 67–83.
Chiodini, G., Cioni, R., Guidi, M., Raco, B., Marini, L., 1998. Soil CO_2 flux measurements in volcanic and geothermal areas. Appl. Geochem. 13, 543–552.
Ciotoli, G., Lombardi, S., Morandi, S., Zarlenga, F., 2005. A multidisciplinary statistical approach to study the relationships between helium leakage and neo-tectonic activity in a gas province. The Vasto Basin, Abruzzo-Molise (central Italy). Am. Assoc. Petrol. Geol. Bull. 88, 355–372.
Ciotoli, G., Lombardi, S., Annunziatellis, A., 2007. Geostatistical analysis of soil gas data in a high seismic intermontane basin: fucino Plain, central Italy. J. Geophys. Res. 112, B05407. https://doi.org/10.1029/2005JB004044.
Ciotoli, G., Sciarra, A., Ruggiero, L., Annunziatellis, A., Bigi, S., 2016. Soil gas geochemical behaviour across buried and exposed faults during the 24 August 2016 central Italy earthquake. Ann. Geophys. 59https://doi.org/10.4401/ag-7242. Fast Track 5.
Cipriani, A., Lugli, F., Martinelli, G., Sciarra, A., 2017. Analisi isotopiche ($^{87}Sr/^{86}Sr$, $\delta^{18}O$, δD e trizio) delle Salse di Nirano. Suppl. ATTI Soc. Nat. Mat. Modena 148, 155–165 ISSN 0365 - 7027.
Coppi, F., 1875. Brevi note sulle Salse Modenesi. Bollettino del R. Comitato Geologico 7–8, 1–7.
Etiope, G., 2004. New directions: GEM – geologic Emissions of Methane, the missing source in the atmospheric methane budget. Atmos. Environ. 38 (19), 3099–3100. https://doi.org/10.1016/j.atmosenv.2004.04.002.
Etiope, G., 2015. Natural Gas Seepage. The Earth's Hydrocarbon Degassing. Springer International Publishing, Switzerland, 978-3-319-14601-0pp. 199. (eBook)). https://doi.org/10.1007/978-3-319-14601-0.
Etiope, G., Lombardi, S., 1995. Evidence for radon transport by carrier gas through faulted clays in Italy. J. Radioanal. Nucl. Chem. 193 (2), 291–300.
Etiope, G., Martinelli, G., Caracausi, A., Italiano, F., 2007. Methane seeps and mud volcanoes in Italy: gas origin, fractionation and emission to the atmosphere. Geophys. Res. Lett. 34, L14303. https://doi.org/10.1029/2007GL030341.
Etiope, G., Feyzullayev, A., Baciu, C.L., 2009. Terrestrial methane seeps and mud volcanoes: a global perspective of gas origin. Mar. Petrol. Geol. 26 (3), 333–344.

Ferrari, C., Vianello, G., 1985. Le salse dell'emilia-romagna. Regione emilia-romagna. Collana Assessorato Ambiente 116–118.
Gasperi, G., Cremaschi, M., Mantovani Uguzzoni, M.P., Cardarelli, A., Cattani, M., Labate, D., 1989. Evoluzione Plio-Quaternaria del margine appenninico modenese e dell'antistante pianura. Note illustrative alla Carta Geologica. Mem. Soc. Geol. It. 39, 431.
Gorgoni, C., 2003. Le salse di Nirano e le altre salse emiliane - I segreti di un fenomeno tra mito e realtà - Comune di Fiorano Modenese. Tip. ABC, Sesto Fiorentino (Firenze), pp. 128.
Gorgoni, C., Bonori, O., Lombardi, S., Martinelli, G., Sighinolfi, G.P., 1988. Radon and helium anomalies in mud volcanoes from northern Apennines (Italy) –a tool for earthquake prediction. Geochem. J. 22, 265–273.
Grassa, F., Capasso, G., Favara, R., Inguaggiato, S., Faber, E., Valenza, M., 2004. Molecular and isotopic composition of free hydrocarbon gases from Sicily, Italy. Geophys. Res. Lett. 31, L06607. https://doi.org/10.1029/2003GL019362.
Heller, C., Blumenberg, M., Kokoschka, S., Wrede, C., Hoppert, M., Taviani, M., Reitner, J., 2011. Geomicrobiology of fluid venting structures at the salse di Nirano mud volcano area in the northern Apennines (Italy). In: In: Reitner, J. (Ed.), Advances in Stromatolite Geobiology, Lecture Notes in Earth Sciences, vol. 131. pp. 209–220. https://doi.org/10.1007/978-3-642-10415-2_14.
Heller, C., Blumenberg, M., Hoppert, M., Taviani, M., Reitner, J., 2012. Terrestrial mud volcanoes of the Salse di Nirano (Italy) as a window into deeply buried organic –rich shales of Plio-Pleistocene age. Sediment. Geol. 263, 202–209. https://doi.org/10.1016/j.sedgeo.2011.05.004.
Henry, P., Le Pichon, X.L., Lallemant, S., Foucher, J.-P., Westbrook, G., Hobart, M., 1990. Mud volcano field seaward of the Barbados Accretionary Complex: a deep-towed scan sonar survey. J. Geophys. Res. 95, 8917–8929.
Hermansson, H.P., Akerblom, G., Chyssler, J., Linden, A., 1991. Geogas, a carrier or a tracer? SKN report 51.
Hinkle, M., 1994. Environmental conditions affecting concentrations of He, CO_2,O_2 and N_2 in soil gases. Appl. Geochem. 9, 53–63.
Hutchinson, G.L., Livingston, G.P., Healy, R.W., Striegl, R.G., 2000. Chamber measurement of surface–atmosphere trace gas exchange: numerical evaluation of dependence on soil, interfacial layer and source/sink properties. J. Geophys. Res. 105, 8865–8875.
Inguaggiato, S., Rizzo, A.L., 2004. Dissolved helium isotope ratios in ground-waters: a new technique based on gas-water re-equilibration and its application to Stromboli volcanic system. Appl. Geochem. 19 (5), 665–673. https://doi.org/10.1016/j.apgeochem.2003.10.009.
Kokoschka, S., Dreier, A., Romoth, K., Taviani, M., Schafer, N., Reitner, J., Hoppert, M., 2015. Isolation of anaerobic bacteria from terrestrial mud volcanoes (salse di Nirano, northern Apennines, Italy). Geomicrobiol. J. 32, 355–364.
Kopf, A., 2002. - Significance of mud-volcanism. Rev. Geophys. 40 (2), 1–52.
Lee, J.Y., Marti, K., Severinghaus, J.P., Kawamura, K., Yoo, H.S., Lee, J.B., Kim, J.S., 2006. A redetermination of the isotopic abundances of atmospheric Ar. Geochem. Cosmochim. Acta 70 (17), 4507–4512.
Lupi, M., Suski Ricci, B., Kenkel, J., Ricci, T., Fuchs, F., Miller, S.A., Kemna, A., 2016. Subsurface fluid distribution and possible seismic precursory signal at the Salse di Nirano mud volcanic field. Italy. Geophys. J. Int. 907–917. https://doi.org/10.1093/gji/ggv454.
Madonia, P., Grassa, F., Cangemi, M., Musumeci, C., 2011. Geomorphological and geochemical characterization of the 11 August 2008 mud volcano eruption at S. Barbara village (Sicily, Italy) and its possible relationship with seismic activity. Nat. Hazards Earth Syst. Sci. 11, 1545–1557.
Mamyrin, B.A., Tolstikhin, I.N., 1984. Helium Isotopes in Nature. Elsevier, Amsterdam.
Manga, M., Bonini, M., 2012. Large historical eruptions at subaerial mud volcanoes, Italy. Nat. Hazards Earth Syst. Sci. 12 (11), 3377–3386. https://doi.org/10.5194/nhess-12-3377-2012.
Martinelli, G., 1999. Mud volcanoes of Italy: a review. Giornale di Geologia, ser. 3 (61), 107–113.
Martinelli, G., Judd, A., 2004. Mud volcanoes of Italy. Geol. J. 39, 49–61.
Martinelli, G., Rabbi, E., 1998. The Nirano mud volcanoes. In: Curzi, P.V., Judd, A.G. (Eds.), Abstracts and Guide Book, Vth International Conference on Gas in Marine Sediments, Bologna, Italy; September 1998. Grafiche A & B, Bologna, pp. 202–206.
Mazzini, A., Etiope, G., 2017. Mud volcanism: an updated review. Earth Sci. Rev. 168, 81–112.
Mazzini, A., Svensen, H., Planke, S., Guliyev, I., Akhmanov, G.G., Fallik, T., Banks, D., 2009. When mud volcanoes sleep: insight from seep geochemistry at the Dashgil mud volcano, Azerbaijan. Mar. Petrol. Geol. 26, 1704–1715. https://doi.org/10.1016/j.marpetgeo.2008.11.003.
Milkov, A.V., Etiope, G., 2018. Revised genetic diagrams for natural gases based on a global dataset of > 20,000 samples. Org. Geochem. 125, 109–120. https://doi.org/10.1016/j.orggeochem.2018.09.002.
Minissale, A., Magro, G., Martinelli, G., Vaselli, O., Tassi, G.F., 2000. Fluid geochemical transect in the Northern Apennines (central-northern Italy):fluid genesis and migration and tectonic implications. Tectonophysics 319, 199–222.
Mucchi, A.M., 1966. Il fenomeno delle salse e le manifestazioni del Modenese. ATTI Soc. Nat. Mat. Modena 97, 1–31.
Mucchi, A.M., 1968. Le salse del Modenese e del Reggiano. L'Universo 48 (3), 421–436.
Ozima, M., Podosek, F.A., 2002. Noble Gas Geochemistry, second ed. Cambridge University Press, Cambridge0-521-80366-7.
Pallasser, R.J., 2000. Recognising biodegradation in gas/oil accumulations through the $\delta^{13}C$ compositions of gas components. Org. Geochem. 31, 1363–1373.
Pantanelli, D., Santi, V., 1896. L'Appennnino Modenese. Ed. Cappelli, Rocca San Casciano, Ristampa 1996, Ed. Iaccheri, Pavullo Nel Frignano.
Pellegrini, M., Brazzorotto, C., Forti, P., Francavilla, F., Rabbi, E., 1982. Idrogeologia del margine pede-appenninico emiliano romagnolo. In: Cremonini, G., Ricci Lucchi, F. (Eds.), –Guida alla geologia del margine appenninico-padano. Guida Geol. Reg. Soc. Geol. It., Bologna, pp. 183–189.
Pieri, M., Groppi, G., 1981. Subsurface geological structure of the Po plain. Italy. Pubbl. 414. Progetto Finalizzato Geodinamica, C.N.R.
Quattrocchi, F., Pizzi, A., Gori, S., Boncio, P., Voltattorni, N., Sciarra, A., 2012. The contribution of fluid geochemistry to define the structural pattern of the 2009 L'Aquila seismic source. Int. J. Geosci. 131, 448–458. ISSN: 2038–1727. https://doi.org/10.3301/IJG.2012.31.
Saunois, M., Bousquet, P., Poulter, B., Peregon, A., Ciais, P., Canadell, J.G., Dlugokecky, E.J., Etiope, G., Bastviken, D., Houweling, S., Janssens-Maenhout, G., et al., 2016. The global methane budget: 2000-2012. Earth Syst. Sci. Data Discuss. https://doi.org/10.5194/essd-2016-25.
Schoell, M., 1980. The hydrogen and carbon isotopic composition of methane from natural gases of various origins. Geochem. Cosmochim. Acta 44, 649–661.
Sciarra, A., Cinti, D., Pizzino, L., Procesi, M., Voltattorni, N., Mecozzi, S., Quattrocchi, F., 2013. Geochemistry of shallow aquifers and soil gas surveys in a feasibility study at the Rivara natural gas storage site (Po Plain, Northern Italy). Appl. Geochem. 34, 3–22. https://doi.org/10.1016/j.apgeochem.2012.11.008.
Sciarra, A., Cantucci, B., Castaldini, D., Procesi, M., Conventi, M., 2015a. Between history, work and passion: medieval castle, mud volcanoes and Ferrari. Geol. F. Trips 7 (n.1.1), 42pp. https://doi.org/10.3301/GFT.2015.01. ISSN 2038-4947.
Sciarra, A., Fascetti, A., Moretti, A., Cantucci, B., Pizzino, L., Lombardi, S., Guerra, I., 2015b. Geochemical and radiometric profiles through an active fault in the Sila Massif (Calabria, Italy). J. Geochem. Explor. 148, 128–137.
Sciarra, A., Cantucci, B., Coltorti, M., 2017. Learning from soil gas change and isotopic signatures during the 2012 Emilia seismic sequence. Sci. Rep. 7, 14187. https://doi.org/10.1038/s41598-017-14500-y.
Sciarra, A., Mazzini, A., Inguaggiato, S., Vita, F., Lupi, A., Hadi, S., 2018. Radon and carbon gas anomalies along the Watukosek fault system and Lusi mud eruption, Indonesia. Mar. Petrol. Geol. 90, 77–90. https://doi.org/10.1016/j.marpetgeo.2017.09.031.
Segovia, N., Seidel, J.L., Monnin, M., 1987. Variations of radon in soils induced by external factors. J. Radioanal. Nucl. Chem. Lett. 119, 199–209.
Sinclair, A.J., 1974. Selection of threshold values in geochemical data using probability graphs. J. Geochem. Explor. 3, 129–149.
Sinclair, A.J., 1991. A fundamental approach to threshold estimation in exploration geochemistry: probability plots revisited. J. Geochem. Explor. 41, 1–22.
Stoppani, A., 1873. Il Bel Paese. Milano. pp. 651.
Tassi, F., Bonini, M., Montegrossi, G., Capecchiacci, F., Capaccioni, B., Vaselli, O., 2012. Origin of hydrocarbons in gases from mud volcanoes and CH_4-rich emissions. Chem. Geol. 294 (295), 113–126.
Tomonaga, Y., Brennwald, M.S., Kipfer, R., 2011. An improved method for the analysis of dissolved noble gases in the pore water of unconsolidated sediments. Limnol Oceanogr. Methods 9, 42–49 doi:10:4319/lom.2011.9.42.
Tomonaga, Y., Brennwald, M.S., Kipfer, R., 2013. Using helium and other noble gases in ocean sediments to characterize active methane seepage off the coast of New Zealand. Mar. Geol. 344, 34–40. https://doi.org/10.1016/j.margeo.2013.07.010.
Tomonaga, Y., Brennwald, M.S., Meydan, A.F., Kipfer, R., 2014. Noble gases in the sediments of Lake Van - solute transport and palaeo-environmental reconstruction. Quat. Sci. Rev. 104, 117–126. https://doi.org/10.1016/j.quascirev.2014.09.005.
Tomonaga, Y., Brennwald, M.S., Kipfer, R., 2015. Attenuation of noble-gas transport in laminated sediments of the Stockholm Archipelago. Limnol. Oceanogr. 60 (2), 497–511. https://doi.org/10.1002/lno.10045.
Tyroller, L., Tomonaga, Y., Brennwald, M.S., Ndayisaba, C., Naeher, S., Schubert, C., North, R.P., Kipfer, R., 2016. Improved method for the quantification of methane concentrations in unconsolidated lake sediments. Environ. Sci. Technol. 50 (13), 7047–7055. https://doi.org/10.1021/acs.est.5b05292.
Valente, E., Ascione, A., Ciotoli, G., Cozzolino, M., Porfido, S., Sciarra, A., 2018. Do moderate magnitude earthquakes generate seismically induced ground effects? The case study of the Mw = 5.16, 29th December 2013 Matese earthquake (southern Apennines, Italy). Int. J. Earth Sci. 107, 517–537. https://doi.org/10.1007/s00531-017-1506-5.
Wang, W.C., Zhang, L.Y., Liu, W.H., Kang, Y., Ren, J.H., 2005. Effects of biodegradation on the carbon isotopic composition of natural gas — a case study in the Bamianhe oil field of the Jiyang Depression, Eastern China. Geochem. J. 39, 301–309.
Whiticar, M.J., Suess, E., 1990. Hydrothermal hydrocarbon gases in the sediments of the king-george basin, bransfield strait, antartica. Appl. Geochem. 5, 135–147.